Motion kinematics analysis of wheeled-legged rover over 3D surface with posture adaptation

Christophe Grand, Faïz Ben Amar, Frédéric Plumet
LRP, University Pierre et Marie Curie - Paris 6,
CNRS FRE 2507, Paris, France

Abstract— *This paper deals with motions kinematics analysis of wheeled-legged mobile robot. A kineto-static modeling of such system is proposed. Based on this general model, we develop the inverse differential kinematics of Hylos robot, a prototype of hybrid wheeled-legged rover developed in our lab. This inverse model is applied to determine a posture control algorithm of the robot evolving on uneven terrain.*

Keywords: **hybrid wheel-legged, mobile robot**

I. Introduction

Autonomous robotic rovers have many potential applications, including space exploration, agriculture, defense, demining, etc... Rovers as Sojourner Shrimp [1] , Nomad [2] are articulated multibody structure permitting a passive adaption to ground surface. New kinematics such as for SRR [3] or Gofor [4] use an active suspension allowing control of some attitude parameters of the robot. Those articulated wheeled systems differs from walking machines in the sense that wheeled systems maintain the contact continuously with the ground surface and velocity transmission is mainly ensured by rolling on ground. High mobility systems such as Azimut [5], Hylos [6], Workpartner, Athlete [7] combining both rolling and crawling, inherits both advantages of wheeled and walking systems, i.e. the velocity for the first one and the clearing for the second.

Numerous works are related to the motion analysis of articulated wheeled systems. Kinematic analysis of motion on flat surface are developed by [8] and [9]. A classification of those systems, based on steering systems including omnidirectional wheels, are proposed in [10]. Those works are based on ideal rolling and no-side slip assumptions. Kinematics of 2 linked wheels by an axle on 3D surface is studied by [11]. This study propose the using a variable length axle to prevent side slip. The rolling kinematic of a torus wheel on uneven continuous surface is investigated in [12] which propose the using a passive joint allowing a lateral degree of freedom in order to overcome slippage. A methodology for developing a motion kinematics over rough ground and including various slip is proposed in [13].

This paper proposes a general kinetostatic formulation of quasi-static motion of articulated wheeled-legged rovers (WLR). This formulation include no-ideal contact condition (rolling slip, side-slip, discontinuous contact, contact deformation). The method used here is based on velocity composition principle to derive velocity equation between which link operational and joint parameters. Virtual work principles is used to derive equilibrium equation and force transmission equations which connect contact force, joint torques and external gravitational forces. Those models are applied for trajectory control of a wheeled-legged rover based on a posture/path decoupling parameters.

Section 2 will present first a general formulation of velocity and forces transmission of WLR. Then those models are applied, in section 3, to our experimental platform composed by four wheel-legs, and are solved in their inverse form which is convenient for posture-trajectory control. Section 4 discusses about the posture control applied to our experimental platform.

II. General kineto-static formulation of WLR

This section deals with kineto-static modeling of systems having legs ended with wheels. We define the parameter vector $\mathbf{q}^{\mathrm{t}} = (\mathbf{x}^{\mathrm{t}}, \boldsymbol{\theta}_{\mathbf{i}}^{\mathrm{t}}, \boldsymbol{\chi}_{\mathbf{i}}^{\mathrm{t}})^{\mathbf{t}}$ such as :

- $\mathbf{x}^{\mathrm{t}} = (\mathbf{p}^{\mathrm{t}}, \boldsymbol{\phi}^{\mathrm{t}})$ is the vector of platform parameters with respect to ground frame, where $\mathbf{p}$ denotes the vector of position parameters and $\boldsymbol{\phi}$ denotes the vector of the usual yaw, pitch and roll angles;
- $\boldsymbol{\theta}_{\mathbf{i}}$ is the vector of the ith leg joint parameters;
- $\boldsymbol{\chi}_{\mathbf{i}} = (\gamma_{\mathbf{i}}, \vartheta_{\mathbf{i}})^{\mathrm{t}}$ is the ith vector of wheel's parameter, where γ_i is the steering angle and ϑ_i the rolling angle.

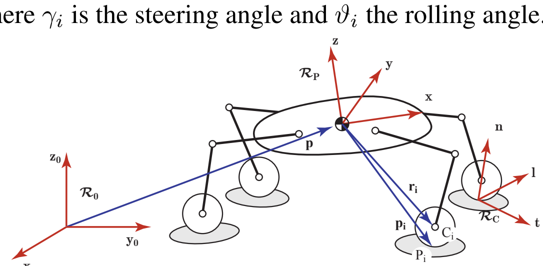

Fig. 1. Kinematic model

Let n the number of wheel-leg kinematic chain and $\mathbf{q}$ the vector of the robot parameters :

$$\mathbf{q}^{\mathrm{t}} = (\mathbf{x}^{\mathrm{t}}, \boldsymbol{\theta}_{\mathbf{1}}^{\mathrm{t}}, \boldsymbol{\chi}_{\mathbf{1}}^{\mathrm{t}}, \boldsymbol{\theta}_{\mathbf{2}}^{\mathrm{t}}, \boldsymbol{\chi}_{\mathbf{2}}^{\mathrm{t}}, \ldots)^{\mathrm{t}}$$

A. Contact model

The contact area between a ground and a wheel could have a complex geometry depending on one part the flexibility of the ground and on the other part their geometry. Figure (2) gives a generic approached form of the contact area between a cylindrical flexible wheel on a soft ground. The center point of the contact area is called P_i and an associated contact frame $\mathcal{R}_\mathrm{i} = (\mathrm{P_i}, \mathbf{t}, \mathbf{l}, \mathbf{n})$ is defined such as $\mathbf{n}$ is the contact normal vector, $\mathbf{t} = \boldsymbol{\sigma} \times \mathbf{n}$ is the longitudinal vector with $\boldsymbol{\sigma}$ is the unit wheel axis and $\mathbf{l} = \mathbf{n} \times \mathbf{t}$ is the lateral vector (figure 2(b)).

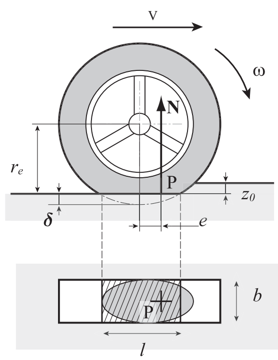

(a) Contact geometry

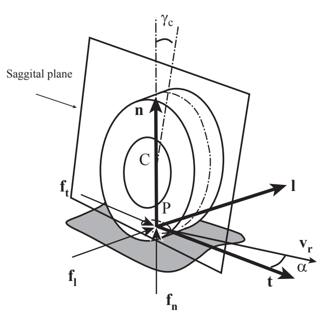

(b) Contact frame

Fig. 2. Contact between a flexible wheel and a soft ground

B. Velocity equations

As the system is mechanically non-holonomic, kinematic equations can not be given geometrically but will be established by using the velocity relations in articulated rigid bodies system. These equations assumes permanent contacts but not necessary ideal rolling with the ground i.e. the wheels could slip in both tangent directions of contact plane. The velocity equation is obtained by means of the velocity composition principle :

$$\begin{aligned} \vec{\mathbf{V}}_{(\mathrm{P_i},\mathcal{R}_{\omega_\mathrm{i}}/\mathcal{R}_0)} &= \vec{\mathbf{V}}_{(\mathrm{P_i},\mathcal{R}_{\omega_\mathrm{i}}/\mathcal{R}_\mathrm{c})} + \\ & \vec{\mathbf{V}}_{(\mathrm{P_i},\mathcal{R}_\mathrm{c}/\mathcal{R}_\mathrm{p})} + \vec{\mathbf{V}}_{(\mathrm{P_i},\mathcal{R}_\mathrm{p}/\mathcal{R}_0)} \end{aligned} \tag{1}$$

Where $\mathcal{R}_0$ is the global frame, $\mathcal{R}_\mathrm{p}$ is the platform frame, $\mathcal{R}_\mathrm{c}$ is the frame attached to the wheel axle and $\mathcal{R}_{\omega_\mathrm{i}}$ is the frame attached to the rotating wheel (see Fig. 1).

This equation is expressed in the contact frame $\mathcal{R}_i$:

$$\mathbf{v_s^i} = -\mathbf{v_c^i} + \mathbf{v_p^i} + \mathbf{v_x^i} \tag{2}$$

where :
- $\mathbf{v_s^i} = \vec{\mathbf{V}}_{(\mathrm{P_i},\mathcal{R}_{\omega_\mathrm{i}}/\mathcal{R}_0)}$ is the sliding velocity of the contact point P_i;
- $\mathbf{v_x^i} = \vec{\mathbf{V}}_{(\mathrm{P_i},\mathcal{R}_\mathrm{p}/\mathcal{R}_0)}$ is the velocity of P_i due to platform motion with respect to ground;
- $\mathbf{v_p^i} = \vec{\mathbf{V}}_{(\mathrm{P_i},\mathcal{R}_\mathrm{c}/\mathcal{R}_\mathrm{p})}$ is the velocity of P_i due to leg's motion with respect the platform;
- $\mathbf{v_c^i} = -\vec{\mathbf{V}}_{(\mathrm{P_i},\mathcal{R}_{\omega_\mathrm{i}}/\mathcal{R}_\mathrm{c})} = r\omega_i \mathbf{t_i}$ is the wheel circumferential velocity with respect to the leg. In this equation, subscript $\mathbf{i}$ denotes that the vector is expressed in the local contact frame $\mathcal{R}_i$.

First, the velocity of the contact point due to platform motion with respect to the ground and expressed in the platform frame $\mathcal{R}_\mathrm{p}$ can be written as :

$$\mathbf{v_x} = \mathbf{R}\dot{\mathbf{p}} + \boldsymbol{\omega} \times \mathbf{p_i} \tag{3}$$

where $\dot{\mathbf{p}}$ is the platform velocity expressed in $\mathcal{R}_0$ and $\boldsymbol{\omega}$ is the platform rotation velocity vector expressed in $\mathcal{R}_\mathrm{p}$. $\mathbf{R}$ is rotation matrix between the platform frame and the ground one and $\mathbf{p_i}$ is the position of the point contact in the platform frame.

The vector $\mathbf{p_i}$ depends on leg parameters $\boldsymbol{\theta}_\mathbf{i}$. It is obtained by writing the kinematic model of the leg :

$$\mathbf{p_i} = \mathbf{r_i} - r\mathbf{n} \approx \mathcal{G}_i(\boldsymbol{\theta}_\mathbf{i}) - r\mathbf{n} \tag{4}$$

Then equation (3) can be rewritten in matrix form :

$$\begin{aligned} \mathbf{v_x} &= \mathbf{R}\dot{\mathbf{p}} - \widetilde{\mathbf{p}}_\mathbf{i}\mathbf{T}_{\boldsymbol{\phi}}\dot{\boldsymbol{\phi}} \\ &= \begin{bmatrix} \mathbf{R} & -\widetilde{\mathbf{p}}_\mathbf{i}\mathbf{T}_{\boldsymbol{\phi}} \end{bmatrix} \dot{\mathbf{x}} \\ &= \mathbf{L_i}\dot{\mathbf{x}} \end{aligned} \tag{5}$$

where $\widetilde{\mathbf{p}}_\mathbf{i}$ is the skew matrix corresponding to the cross-product, $\dot{\mathbf{x}}$ is the platform velocity twist with respect to the ground frame $\mathcal{R}_0$ and $\mathbf{T}_{\boldsymbol{\phi}}$ is the rotation velocity decoupling matrix. This matrix expresses the rotation velocity vector $\boldsymbol{\omega}$ as a function of the rotation angle derivative $\dot{\boldsymbol{\phi}}$. $\mathbf{L_i}$ is called locomotion matrix with a 3×6 dimensions.

The velocity of the contact point $\mathrm{P_i}$ due to leg motion with respect to the platform is expressed by classical serial chain kinematic model :

$$\begin{aligned} \mathbf{v_{p_i}} &= \mathbf{J_{p_i}}\dot{\boldsymbol{\theta}}_\mathbf{i} \\ &= \begin{bmatrix} \boldsymbol{\sigma}_\mathbf{1} \times \mathbf{a_1} & \dots & \boldsymbol{\sigma}_\mathbf{m} \times \mathbf{a_m} \end{bmatrix} \dot{\boldsymbol{\theta}}_i \end{aligned} \tag{6}$$

We then obtain from equation (2) by projection on the contact frame :

$$\mathbf{R_i^t}\mathbf{L_i}\dot{\mathbf{x}} + \mathbf{R_i^t}\mathbf{J_{p_i}}\dot{\boldsymbol{\theta}}_\mathbf{i} - r\,\omega_i(1,0,0)^\mathbf{t} = \mathbf{v_{s_i}} \tag{7}$$

$\mathbf{R_i}$ is matrix rotation of contact frame with respect to platform frame. The projection in the contact frame allows to express directly the sliding condition in the contact. By denoting $\mathbf{v}_{s_i} = [s_{t_i} \;\; s_{l_i} \;\; s_{n_i}]^t$ the relative velocity in the contact:

- s_{t_i} expresses the longitudinal slippage velocity,
- s_{l_i} expresses the lateral slippage velocity,
- s_{n_i} represent contact deformation velocity in the normal direction or contact detachment velocity.

Finally, we obtain, in matrix-form, the velocity equation for the all system composed by n wheel-leg chains:

$$\mathbf{L}(\mathbf{x}, \mathbf{\Theta}, \mathbf{n})\dot{\mathbf{x}} + \mathbf{J}(\mathbf{\Theta}, \mathbf{n})\dot{\mathbf{\Theta}} = \mathbf{v_s} \tag{8}$$

with

$$\mathbf{L} = \begin{bmatrix} \mathbf{R}_1^{\mathrm{t}}\mathbf{L_1} \\ \mathbf{R}_2^{\mathrm{t}}\mathbf{L_2} \\ \vdots \\ \mathbf{R}_n^{\mathrm{t}}\mathbf{L_n} \end{bmatrix}_{\mathbf{3n\times 6}} \qquad \mathbf{J} = \begin{bmatrix} \mathbf{J_1} & \mathbf{0} & \dots & \mathbf{0} \\ \mathbf{0} & \mathbf{J_2} & & \mathbf{0} \\ \vdots & & \ddots & \\ \mathbf{0} & \mathbf{0} & & \mathbf{J_n} \end{bmatrix}_{3n\times n\,m}$$

$$\mathbf{\Theta} = \begin{bmatrix} \boldsymbol{\theta_1} \\ \boldsymbol{\chi_1} \\ \boldsymbol{\theta_2} \\ \boldsymbol{\chi_2} \\ \vdots \\ \boldsymbol{\theta_n} \\ \boldsymbol{\chi_n} \end{bmatrix}_{n\,m\times 1} \qquad \mathbf{J_i} = \begin{bmatrix} \mathbf{R}_i^{\mathrm{t}}\mathbf{J_{P_i}} & \begin{bmatrix} -r \\ 0 \\ 0 \end{bmatrix} \end{bmatrix}_{3\times m}$$

by assuming that all chains have the same degree of freedom m. The Jacobian matrix $\mathbf{J_i}$ of each wheel-leg chain depends on the normal vectors of wheel-ground contacts $\mathbf{n}^{\mathrm{t}} = (\mathbf{n}_1^{\mathrm{t}}, \mathbf{n}_2^{\mathrm{t}}, \dots, \mathbf{n}_n^{\mathrm{t}})$.

C. Quasi-static model

We denotes $\mathbf{f}^{\mathrm{t}} = (\mathbf{f}_1^{\mathrm{t}}, \mathbf{f}_2^{\mathrm{t}}, ..., \mathbf{f}_n^{\mathrm{t}})$ with $\mathbf{f_i} = (\mathbf{f_{t_i}}, \; \mathbf{f_{l_i}}, \; \mathbf{f_{n_i}})^{\mathrm{t}}$ the vector of contact force components. We will use the principle of virtual power to determine the static equation assuming a virtual velocity field $(\dot{\mathbf{x}}^*, \; \dot{\mathbf{\Theta}}^*, ^{\mathrm{t}} \mathbf{v}_\mathbf{s}^*)$ which must satisfies kinematic equation 8:

$$P^* = \mathbf{w}^{\mathrm{t}}\dot{\mathbf{x}}^* + \boldsymbol{\tau}^{\mathrm{t}}\dot{\mathbf{\Theta}}^* + \mathbf{f}^{\mathrm{t}}\mathbf{v}_\mathbf{s}^* = \mathbf{0} \tag{9}$$

Let $\mathbf{w}$ the vector 6×1 of the wrench components, expressed in the platform frame center, of external forces applied to the system (including gravitational forces). We denote $\boldsymbol{\tau}$ the actuator torque vector applied on joints. The total power developed by external forces, contact forces and joint torques is:

$$\begin{aligned} P^* &= \mathbf{w}^{\mathrm{t}}\dot{\mathbf{x}}^* + \boldsymbol{\tau}^{\mathrm{t}}\dot{\mathbf{\Theta}}^* + \mathbf{f}^{\mathrm{t}}(\mathbf{L}\dot{\mathbf{x}}^* + \mathbf{J}\dot{\mathbf{\Theta}}^*) \\ &= (\mathbf{w}^{\mathrm{t}} + \mathbf{f}^{\mathrm{t}}\mathbf{L})\dot{\mathbf{x}}^* + (\boldsymbol{\tau}^{\mathrm{t}} + \mathbf{f}^{\mathrm{t}}\mathbf{J})\dot{\mathbf{\Theta}}^* \end{aligned} \tag{10}$$

The principle of virtual power states that :

$$P^* = 0 \;\forall(\dot{\mathbf{x}}^*, \; \dot{\mathbf{\Theta}}^*) \Leftrightarrow \begin{cases} -\mathbf{L}^{\mathrm{t}}\mathbf{f} = \mathbf{w} \\ -\mathbf{J}^{\mathrm{t}}\mathbf{f} = \boldsymbol{\tau} \end{cases} \tag{11}$$

These equations assumes that the total mass of the system is concentrated on the platform. The second equation should be corrected by adding $\mathbf{w_s}$ which is the generalized force due to the weight of wheel-leg parts and associated to $\dot{\mathbf{\Theta}}$ parameters:

$$-\mathbf{J}^{\mathrm{t}}\mathbf{f} = \boldsymbol{\tau} + \mathbf{w_s} \tag{12}$$

The system has a high degree of static indeterminacy i.e. equilibrium equations are less than unknown contact forces. This indeterminacy is due in one part to external contact with the environment (frictional contacts with 3 unknown force components at each contact) and in the another part to internal redundant actuation (for example all wheels are in general driven in off-road application). The resolution of this model gives the contact load distribution which are important for determining the traction torque applied to the wheel. In order to solve this model, we have to add relationships or assumptions generally on contact forces. Waldron [14] proposes to use the zero interaction principle to raise the static indeterminacy, based on a equi-projectivity of tangential contact forces. This principle establishes that all tangential contact forces work in the same direction to propel the vehicle. The second way to overcome the indeterminacy is to use terramechanics relations that express relationships between contact force components, slippage parameters and mechanical properties of the ground [15].

III. Application to the inverse velocity model

In this section, we will focus on the particular kinematics of Hylos robot.Then, we will use pure rolling assumption in order to compute the inverse velocity model which will be used in the posture control loop.

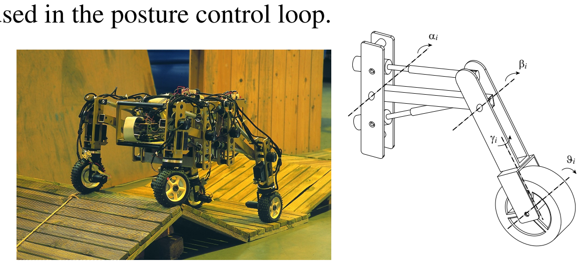

Fig. 3. Hylos robot and CAD view of one wheel-leg

A. Hylos kinematics

Hylos is approximately 70 cm long et weights 12 kg. It is composed by four legs, each one has two rotoide joints with parallel axes and is ended by a driven and steered cylindrical wheel. Leg joints are actuated by means of ball screws and pantographic mechanisms. The system has at all 16 degrees of freedom actuated by DC motors. The figure 3 shows the pantagraphic mechanisms of each 2 dof leg. The leg parameters vector is : $\boldsymbol{\theta_i} = [\alpha_i, \, \beta_i]^{\mathrm{t}}$.

B. Hylos mobility

Ideal rolling assumption deals with non-slippage condition in wheel-ground contact. The inverse kinematic problem consists in determination of the joint velocity for a given desired operational trajectory. The operational parameters should be defined as function of the general mobility of the system, which will be first investigated in this section.

The non slippage condition leads to:

$$\mathbf{L}\dot{\mathbf{x}} + \mathbf{J}\dot{\mathbf{\Theta}} = \mathbf{0} \qquad \textbf{or} \qquad \mathbf{A}\dot{\boldsymbol{q}} = \mathbf{0} \tag{13}$$

with $\mathbf{A} = [\mathbf{L} \mid \mathbf{J}]$ and $\dot{\boldsymbol{q}} = [\dot{\mathbf{x}}\ \dot{\mathbf{\Theta}}]^t$.

An ideal rolling contact is equivalent to an instantaneous spherical joint located in the contact point, so it can be approached as a 3 dof joint. Then we obtain a structure with 18 bodies (including ground) and 20 joints with 28 dof at all. The general Gruebler mobility index is :

$$m_g = 28 - 6(20 - 18 + 1) = 10 \tag{14}$$

This mobility index can also be computed from equation (13) as it is the difference between the 12 equations and the 22 (=6+16) velocity parameters.

However, this general index does not consider the rank of the kinematic equation system and the geometry of joint axes. The real mobility index i.e. the number of independent velocity parameters in the equation (13) can be defined as :

$$m_r = \dim(\mathbf{q}) - \mathbf{rank}(\mathbf{A}) \tag{15}$$

Figure (4) depicts real kinematic mobility index as function of contact normals and rover configurations. For a general configuration of the robot and the ground, this mobility is equal to 10, i.e. all equations in (13) are independents. However, some particular configurations exhibit higher mobility (11 or 12), where the rank of matrix $\mathbf{A}$ is equal to (11 or 10). In these cases, mobility increases and represents a partial internal mobility of the steering axes where the joint velocities become independents of all other vehicle velocity parameters. In theses configurations, the additional mobilities seem to be located in the steering axes which are in theses cases collinear to the contact normals.

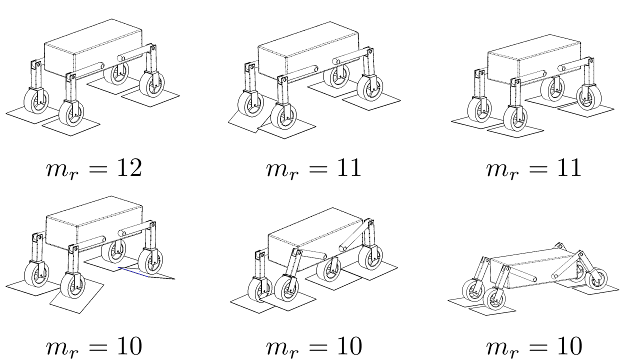

Fig. 4. Mobility for some cases as function of contact planes and of configurations

C. Velocity space reduction

As said in the previous section, the velocity parameter of the steering axis is independent of other velocity parameters when the steering axis is colinear to the contact normal. This configuration introduces a singularity in the Jacobian matrix as the steering axis passes through the contact point. For other configurations (mainly depending of the caster angle between the steering axis and the contact normal), the column of $\mathbf{J_i}$, of equation (8), associated to the steering rate $\dot{\gamma}_i$ is almost $\mathbf{0}$ which leads to an ill-conditioned matrix. Furthermore, the called caster angle must be as small as possible in order to keep the contact area on the rolling tread of the cylindrical wheel during steering. Then, this column of the jacobian matrix and the associated time-derivative rate will be removed in the following development. In parallel to this, we will split velocity equations in two groups :

- The first one corresponds to other kinematic constraint i.e. longitudinal non-slippage condition $\mathbf{t_i^t v_{s_i}} = \mathbf{0}$ and permanent contact condition $\mathbf{n_i^t v_{s_i}} = \mathbf{0}$.
- The second one corresponds to lateral slippage constraints $\mathbf{l_i^t v_{s_i}} = \mathbf{0}$,

The first group can be written by

$$\mathbf{B_x L}\dot{\mathbf{x}} + (\mathbf{B_x J B_j^t})(\mathbf{B_j}\,\dot{\mathbf{\Theta}}) = \mathbf{0} \tag{16}$$

with

$$\mathbf{B_x} = \left[\begin{array}{ccc} \begin{bmatrix} 1 & 0 & 0 \\ 0 & 0 & 1 \end{bmatrix} & & \mathbf{0} \\ & \ddots & \\ \mathbf{0} & & \begin{bmatrix} 1 & 0 & 0 \\ 0 & 0 & 1 \end{bmatrix} \end{array}\right]_{2n\times 3n}$$

a reduction matrix selecting equation along the $\mathbf{t_i}$ and $\mathbf{n_i}$ axis and

$$\mathbf{B_j} = \left[\begin{array}{ccc} \begin{bmatrix} \mathbf{I} & 0 & 0 \\ 0 & 0 & 1 \end{bmatrix} & & \mathbf{0} \\ & \ddots & \\ \mathbf{0} & & \begin{bmatrix} \mathbf{I} & 0 & 0 \\ 0 & 0 & 1 \end{bmatrix} \end{array}\right]_{(l-n)\times m}$$

a selection matrix eliminating $\dot{\gamma}_i$ parameters and the associated column in the jacobian matrix $\mathbf{J}$.

The second group can be written by

$$\mathbf{B_\gamma L}\dot{\mathbf{x}} + (\mathbf{B_\gamma J B_j^t})(\mathbf{B_j}\,\dot{\mathbf{\Theta}}) = \mathbf{0} \tag{17}$$

with

$$\mathbf{B_\gamma} = \left[\begin{array}{ccc} \begin{bmatrix} 0 & 1 & 0 \end{bmatrix} & & \mathbf{0} \\ & \ddots & \\ \mathbf{0} & & \begin{bmatrix} 0 & 1 & 0 \end{bmatrix} \end{array}\right]_{n\times 3n}$$

a reduction matrix selecting equation along the $\mathbf{l_i}$ axis.

This separation is done in order to separate the resolution of the inverse kinematic problem. First, we will solve the first group by computing the reduced command vector $\mathbf{u} = \mathbf{B_j}\,\dot{\mathbf{\Theta}} = (\dot{\alpha_1}, \dot{\beta_1}, \omega_1, ..., \dot{\alpha_4}, \dot{\beta_4}, \omega_4)$ for a given desired twist components of the platform. Then, in a second phase, we will compute the steering angle γ_i for each wheel which provides the desired motion direction of the platform.

D. Computing joint rate

By analyzing the first equation group based on equation (16), we have to compute 12 joint velocities $\mathbf{u}$ from 6 operational parameters $\dot{\mathbf{x}}$ by using 8 independent equations. Then 10 parameters are free. That means that the system is redundant and there is an infinite solution set for $\mathbf{u}$ that produces a desired motion $\dot{\mathbf{x}}$. We propose to define a new operational vector $\boldsymbol{\xi}^{\mathrm{t}} = (\mathbf{x}^{\mathrm{t}}, \mathbf{e}^{\mathrm{t}})$ of dimension 10 based on the 6 platform parameters and 4 new internal parameters $\mathbf{e} = (e_1, e_2, e_3, e_4)^{\mathrm{t}}$ which are the half wheelbases $e_i = \mathbf{x^t r_i}$.

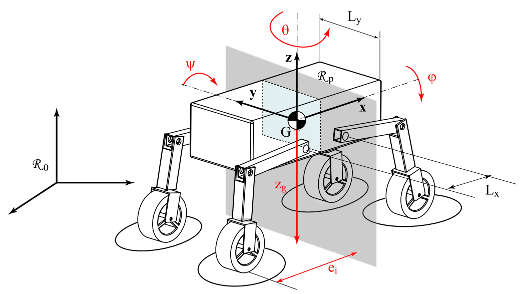

Fig. 5. Hylos parameters and posture definition

$\mathbf{e}$ could be written as function of the command vector $\mathbf{u}$ by analyzing the kinematic wheel-leg chain

$$\dot{\mathbf{e}} = \mathbf{J_e}(\boldsymbol{\Theta})\mathbf{u} \tag{18}$$

This equation expresses the contact point motion as function of the only the leg motion (without the wheel rate). It could be simply deduced from the wheel-leg Jacobian matrix $\mathbf{J_{p_i}}$ defined in equation 6 :

$$\mathbf{J_e}(\boldsymbol{\Theta}) = \begin{bmatrix} \mathbf{j_1} & \mathbf{0} & \mathbf{0} & \mathbf{0} \\ \mathbf{0} & \mathbf{j_2} & \mathbf{0} & \mathbf{0} \\ \mathbf{0} & \mathbf{0} & \mathbf{j_3} & \mathbf{0} \\ \mathbf{0} & \mathbf{0} & \mathbf{0} & \mathbf{j_4} \end{bmatrix}_{4\times 12} \tag{19}$$

with

$$\mathbf{j_i} = [\, l_1 \sin\alpha_i + l_2 \sin(\alpha_i+\beta_i) \quad -l_2\sin(\alpha_i+\beta_i) \quad 0\,]_{1\times 3}$$

Then, we obtain 12 equations system :

$$\widetilde{\mathbf{L}}\dot{\boldsymbol{\xi}} + \widetilde{\mathbf{J}}\mathbf{u} = \mathbf{0} \tag{20}$$

with

$$\widetilde{\mathbf{L}} = \begin{bmatrix} \mathbf{B_x L} \\ \mathbf{I} \end{bmatrix} \quad \text{et} \quad \widetilde{\mathbf{J}} = \begin{bmatrix} \mathbf{B_x J B_j^t} \\ \mathbf{J_e} \end{bmatrix}$$

$\widetilde{\mathbf{J}}$ is square 12x12 and a regular matrix (except some singular cases solved separately), then :

$$\mathbf{u} = -\widetilde{\mathbf{J}}^{-1}\widetilde{\mathbf{L}}\dot{\boldsymbol{\xi}} \tag{21}$$

E. Computing the steering angles

Each equation of the second group (Eq.17) could be solved separately in order to gives the steering angles which are compatible with the desired velocities of the platform $\dot{\mathbf{x}}$ and the other internal velocities $\dot{\theta}$ computed in the last section. Assuming that the lateral contact vector $\mathbf{l_i}$ colinear the wheel axis (i.e. no camber angle), we show easily from equation (17) that

$$\tan\gamma_i = \frac{v_i}{u_i} \tag{22}$$

with

$$\begin{aligned} v_i &= v_y + \omega'_z x_i - \omega'_x z_i \\ u_i &= (v_x + \omega'_y z_i - \omega'_z y_i + \dot{x}_i)\sin(\alpha_i+\beta_i) + \ldots \\ &\quad (v_z + \omega'_x y_i - \omega'_y x_i + \dot{z}_i)\cos(\alpha_i+\beta_i) \end{aligned} \tag{23}$$

and $\mathbf{v} = (v_x, v_y, v_z)^{\mathrm{t}}$ et $\boldsymbol{\omega}' = (\omega'_x, \omega'_y, \omega'_z)^{\mathrm{t}}$ are platform twist parameters in the local frame, then $\mathbf{v} = \mathbf{R}^{\mathrm{t}}\dot{\mathbf{p}}$, $\boldsymbol{\omega}' = \mathbf{R}^{\mathrm{t}}\mathbf{T}_\phi\dot{\boldsymbol{\phi}}$.

For a classical wheeled system moving on a plane, the steering angle is related directly to the lateral velocity of the platform v_y and its yaw rate ω'_z. This is observed in the numerator of the later equation. However, the term $-\omega'_x z_i$ is not usual. In fact, roll platform reconfiguration $-\omega'_x$ needs a roll motion with a non-null steering angle.

IV. Velocity based posture control

In the section, the inverse velocity model is applied to control the posture of the robot evolving in on uneven terrain. Assuming that lateral non-slippage conditions are satisfied by controlling the suitable steering angles at each contact. Equations (21) and (22) allow to control the rover state vector $\boldsymbol{\xi}$ through a linearized state feedback control law.

A. Posture definition

The state vector $\boldsymbol{\xi}^{\mathrm{t}} = (\mathbf{x}^{\mathrm{t}}, \mathbf{e}^{\mathrm{t}}) = (\mathbf{x}, \mathbf{y}, \mathbf{z}, \varphi, \psi, \theta)$ can be split in two set of parameters : 3 parameters (x, y, θ) of the platform horizontal trajectory and 7 posture parameters. These posture parameters correspond to 3 platform attitude parameters (z, ϕ, ψ) and 4 internal parameters (e_1, e_2, e_3, e_4) defined previously by the half wheelbases of each contact. Then the posture parameters vector is defined as:

$$\mathbf{p} = (\varphi,\ \psi,\ \mathbf{z},\ \mathbf{e_1},\ \mathbf{e_2},\ \mathbf{e_3},\ \mathbf{e_4})^{\mathbf{t}}$$

The problem of posture optimization could be treated by considering various performance criteria as stability, traction, energy consumption... . However, it is difficult to estimate contact normal vectors and thus to carry out a real-time efficient optimization of contact force distribution. But, one obvious posture vector could be defined by a constant attitude of the platform (zero pitch and roll angles and a nominal ground clearance z_n) and a constant nominal wheelbases e_n : $\mathbf{p_n} = (\mathbf{0},\ \mathbf{0},\ \mathbf{z_n},\ \mathbf{e_n},\ \mathbf{e_n},\ \mathbf{e_n},\ \mathbf{e_n})^{\mathbf{t}}$

This posture is a good compromise : it preserves stability, ground clearance and force transmission from actuator to contact.

B. Posture control

When the robot crosses an irregular surface, it must maintain its posture around a desired posture $\mathbf{p^d}$. We use a state feedback proportional law for posture control:

$$\dot{\mathbf{p}} = \mathbf{K_p}\left(\mathbf{p^d} - \mathbf{p}\right) \tag{24}$$

where $\dot{\mathbf{p}} = (\dot{\varphi},\ \dot{\psi},\ \dot{z}_g,\ \dot{x_1},\ \dot{x_2},\ \dot{x_3},\ \dot{x_4})^t$ and $\mathbf{K_p}$ a diagonal positive matrix.

Then, we can compute the platform posture velocity by using the following equations:

$$\begin{cases} v_z = -\dot{z}_g + \omega_y \frac{\sum_i x_i}{4} - \omega_x \frac{\sum_i y_i}{4} \simeq -\dot{z}_g \\ \omega_x = \dot{\varphi} - \dot{\theta}\sin\psi \simeq \dot{\varphi} \\ \omega_y = \dot{\psi}\cos\varphi + \dot{\theta}\cos\psi\sin\varphi \simeq \dot{\psi}\cos\varphi \end{cases}$$

The first equation assumes that the projection of the contact center on the horizontal plane is closer the one of the platform center. The two other equations, we neglect the effect of yaw velocity $\dot{\theta}$.

Those posture parameters and the other velocities parameters $(v_x\ , v_y\ , \dot{\theta})^t$ given by path tracking control are used in the inverse velocity model which have to compute from equations (21, 22) the actuator velocity inputs (except for steering actuator, which are controlled in position). On must notice that those equations require the knowledge of normals $\mathbf{n}_i$ at each contact. The equation (7) shows that tangential vector $\mathbf{t}_i$ can be determined from the measure of the system velocity parameters, including platform parameters and joint ones $(\dot{\alpha}_i,\ \dot{\beta}_i)$. However, measuring the 3 components of the instantaneous linear velocity is not simple. In our experiment, we make an estimation of contact normals from the average contact plane.

Our model suppose that wheel-soil contacts are maintained continuously. This function is guaranteed by adding a correction term in the control law:

$$\mathbf{v_{si}^t n_i} = K_f(f_{n_i} - f_0)$$

where f_{n_i} is contact normal force, f_0 is reference value of the contact force (equal to the total weight divided by 4) and K_f is positive matrix.

This control law was implemented on the robot Hylos and experimentally evaluated on the irregular asymmetrical ground profile shown in figure (6). The associated graph depicts the evolution of the rover pitch and roll angles when the robot is moving on this terrain.

V. Conclusion

In this article, we develop the kineto-static model of a wheeled-legged rover. A method to inverse the differential kinematic model had been proposed, this method introduces internal parameters to take the system redundancy

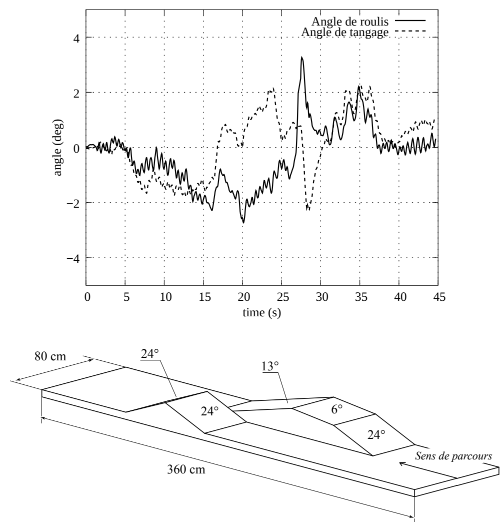

Fig. 6. Corrected pitch and roll angles of the rover evolving on irregular terrain

into account. Posture parameters were introduced and an algorithm for their control had been described. This algorithm uses the inverse velocity model and it was validated for the control of a constant nominal posture.

References

[1] R. Siegwart, P.Lamon, T. Estier, M. Lauria, and R. Piguet. Innovative design for wheeled locomotion in rough terrain. *Robotics and Autonomous Systems*, 40:151–162, 2002.

[2] E. Rollins, J. Luntz, A. Foessel, B. Shamah, and W.L. Whittaker. Nomad: A demonstration of the transforming chassis. In *Proc. of the Int. Conf. on Intelligent Components for Vehicles*, March 1998.

[3] K. Iagnemma, K. Rzepniewski, S. Dubowsky, and P. Schenker. Control of robotic vehicles with actively articulated suspensions in rough terrain. *Autonomous Robots*, 14(1), 2003.

[4] S.V. Sreenivasan and B.H. Wilcox. Stability and traction control of an actively actuated microrover. *Journal of Robotics Systems*, 11(6):487–502, 1994.

[5] F. Michaud et al. Multi-modal locomotion robotic platform using leg-track-wheel articulations. *Autonomous Robots*, 18(2):137, 2005.

[6] Ch. Grand, F. BenAmar, F. Plumet, and Ph. Bidaud. Stability and traction optimisation of high mobility rover. *The International Journal of Robotics Research*, 23(10-11):1041–1058, Oct. 2004.

[7] Kr. Hauser, T. Bretl, J-C Latombe, and B. Wilcox. Motion planning for a six-legged lunar robot. In *Proc. of the The Seventh Int. Workshop on the Algorithmic Foundations of Robotics*, 2006.

[8] P. Muir and C. Neuman. Kinematic modeling of wheeled mobile robots. *Journal of robotics systems*, 4(2):281–340, 1987.

[9] J.C. Alexander and J.H. Maddocks. On the kinematics of wheeled mobile robot. *Int. Journal of Robotics Research*, 8(5):15–27, 1989.

[10] G. Campion, G. Bastin, and B. d'Andra-Novel. Structural properties and classification of kinematic and dynamic models of wheeled mobile robots. *IEEE Trans. on Robotics and Automation*, 12(1):47–62, 1996.

[11] B.J. Choi and S.V. Sreenivasan. Gross motion characteristics of articulated mobile robots with pure rolling capability on smooth uneven surfaces. *IEEE Trans. on Robotics and Automation*, 15(2), 1999.

[12] N. Chakraborty and A. Ghosal. Kinematics of wheeled mobile robots on uneven terrain. *Mechanism and Machine Theory*, 39, 2004.

[13] M. Tarokh and G. J. McDermott. Kinematics modeling and analyses of articulated rovers. *IEEE Trans. on Robotics and Automation*, 21(4):539–554, 2005.

[14] V. Kumar and K. Waldron. Force distribution in closed kinematic chains. *IEEE Trans. on Robotics and Automation*, 4(6):657–663, 1988.

[15] M.G. Bekker. *Introduction to terrain-vehicle systems*. The University of Michigan Press, 1969.